Electronic Supplementary Information on

Type of Complex – BSA Binding Forces Affected by Different Coordination Modes of Alliin in Novel Water-Soluble Ruthenium Complexes

Adnan Zahirović,[1] Dijana Žilić,[2] Sandra Kraljević Pavelić,[3] Mirsada Hukić,[4] Senada Muratović,[2] Anja Harej[3] and Emira Kahrović[1]*

[1] Laboratory for Inorganic and Bioinorganic Chemistry, Department of Chemistry, Faculty of Science, University of Sarajevo, Sarajevo, Bosnia and Herzegovina

[2] Ruđer Bošković Institute, Zagreb, Croatia

[3] Department of Biotechnology, Centre for High-Throughput Technologies, University of Rijeka, Rijeka, Croatia

[4] Institute for Biomedical Research and Diagnostics Nalaz, Sarajevo, Bosnia and Herzegovina

Contents

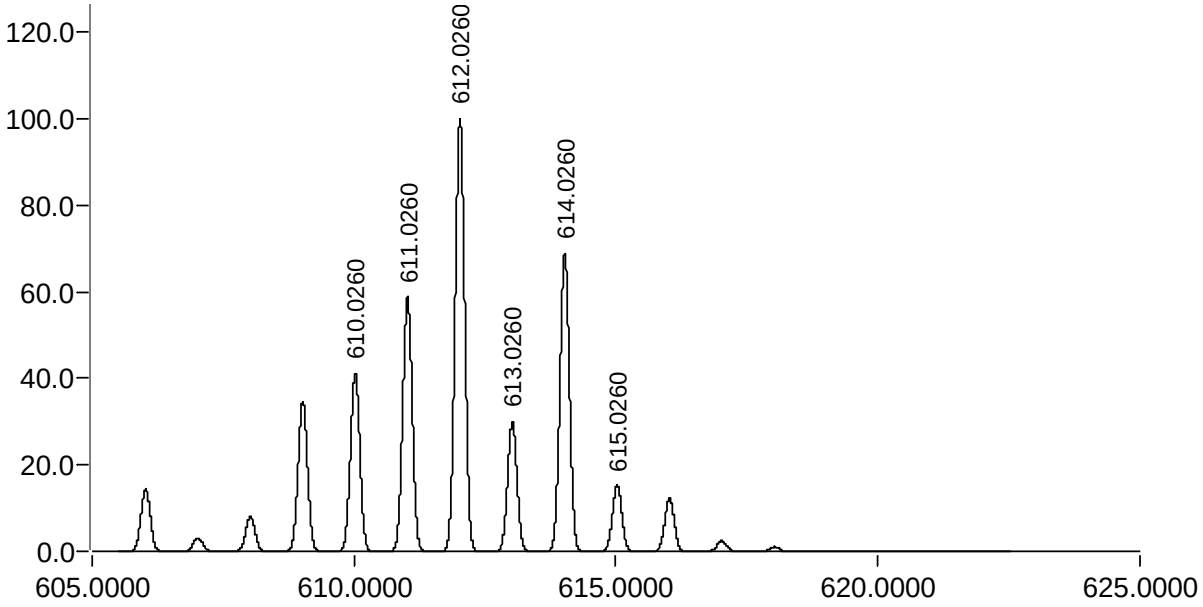

Figure S1. Theoretical isotopic distribution for molecular ion of the complex (**1**).

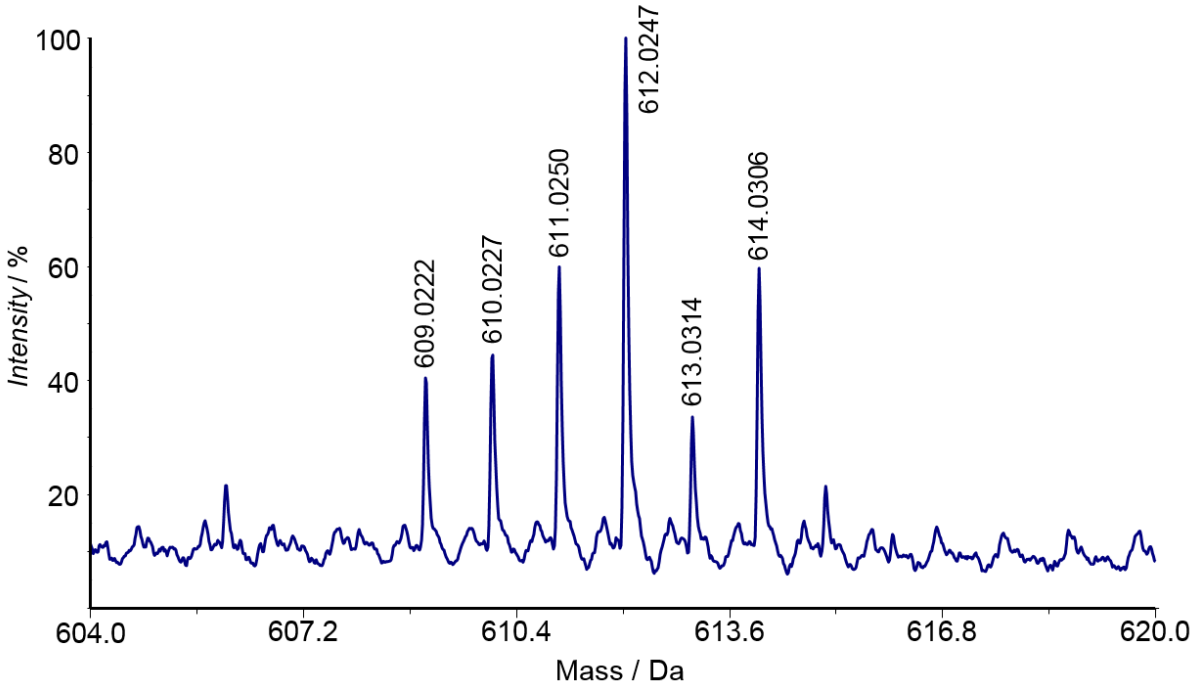

Figure S2. Measured isotopic distribution for molecular ion of the complex (**1**).

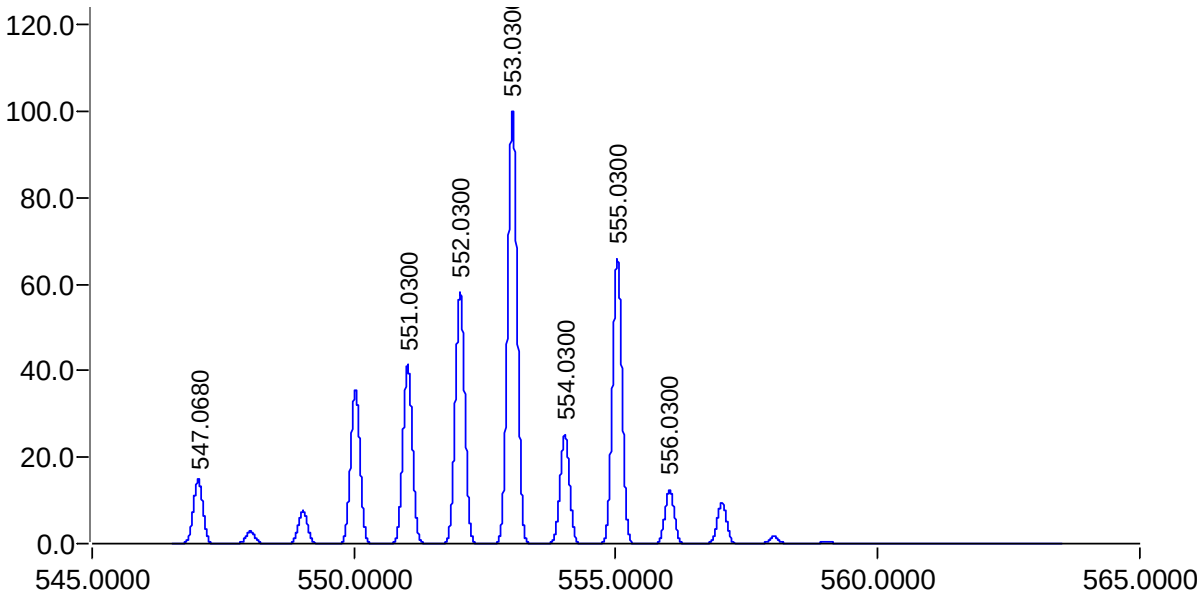

Figure S3. Theoretical isotopic distribution for molecular ion of the complex (**2**).

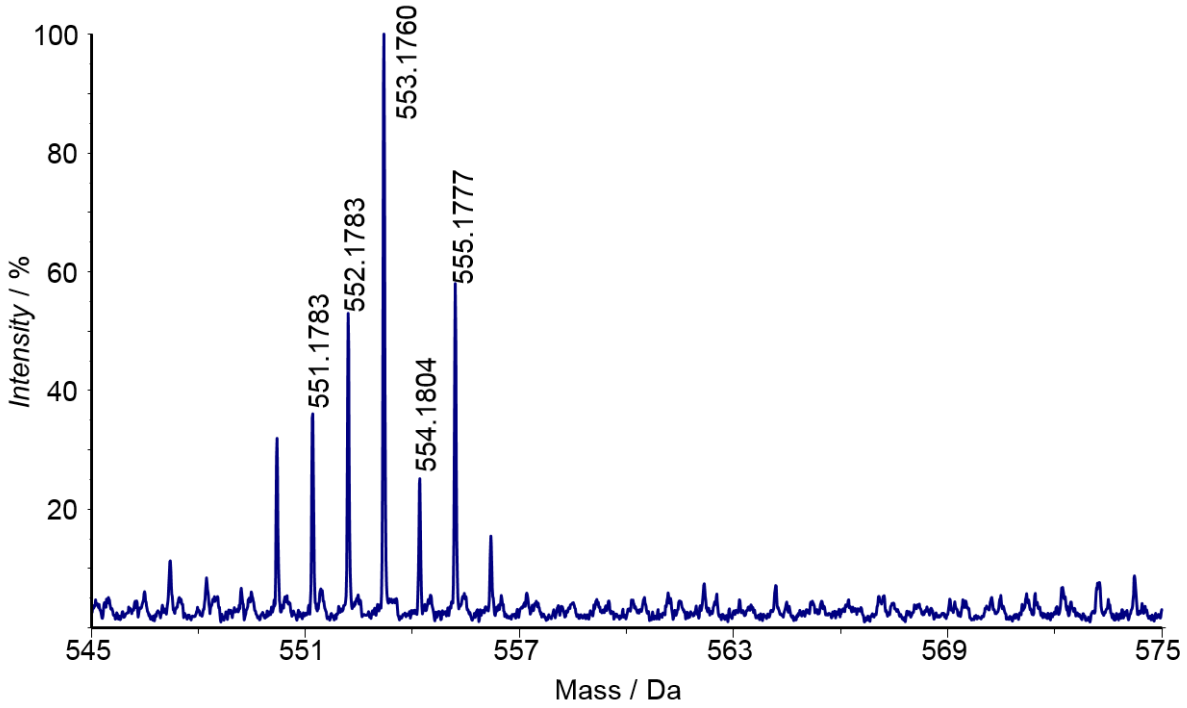

Figure S4. Measured isotopic distribution for molecular ion of the complex (**2**).

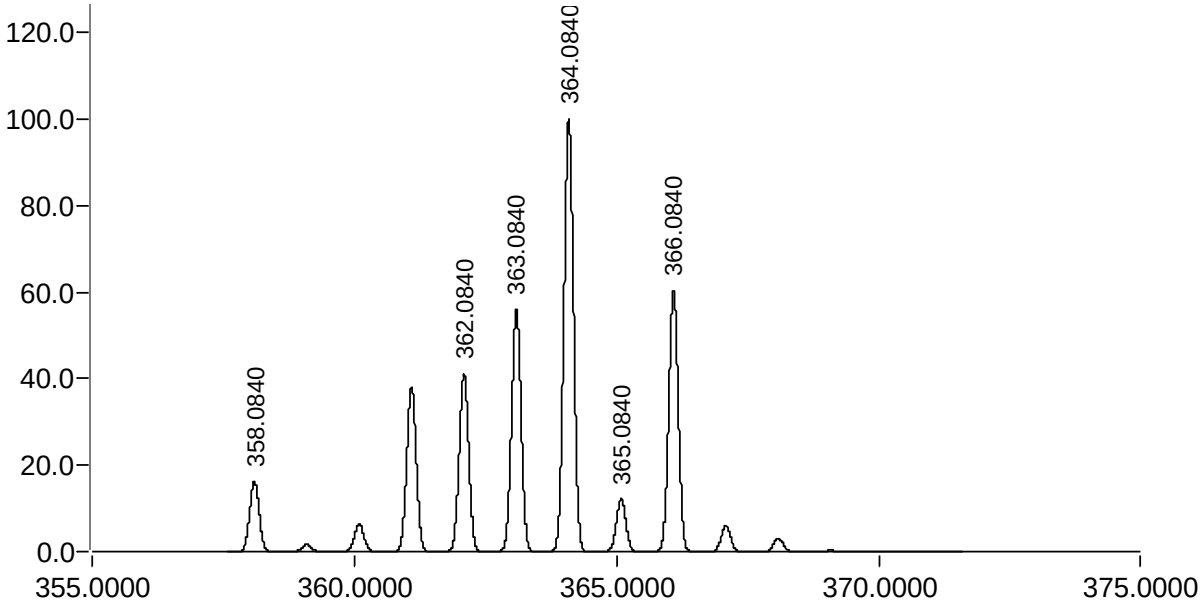

Figure S5. Theoretical isotopic distribution for molecular ion of the complex (**3**).

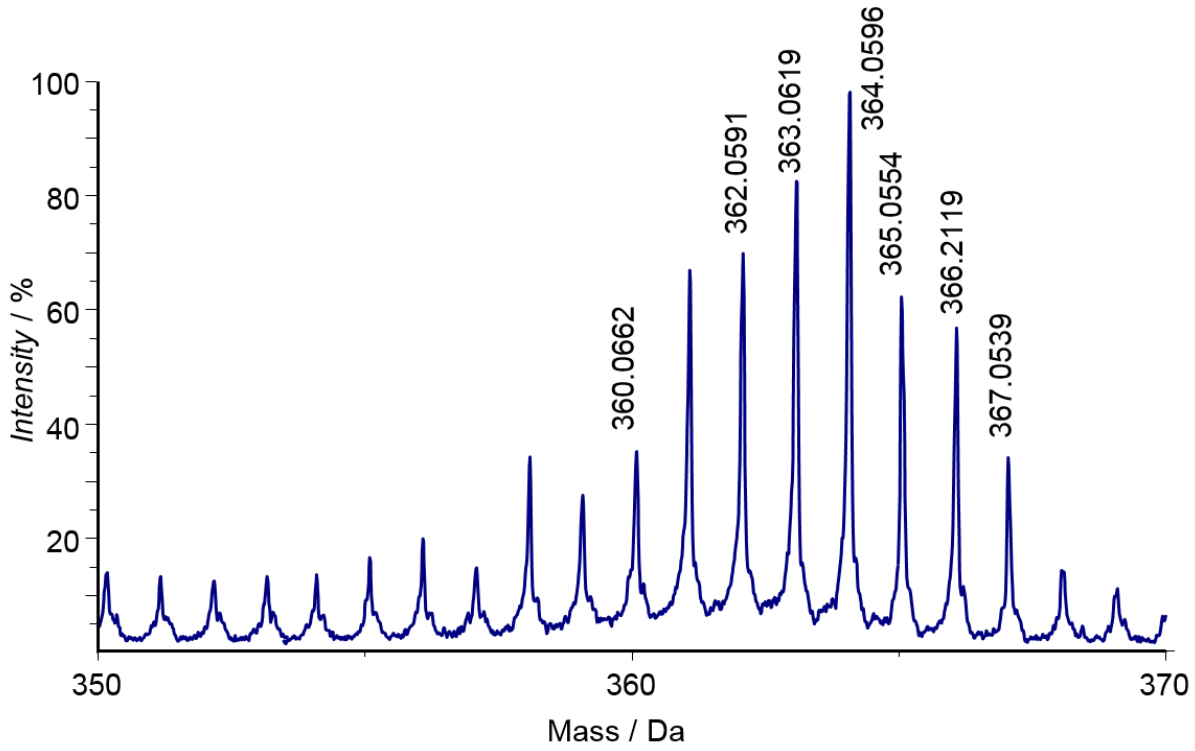

Figure S6. Measured isotopic distribution for molecular ion of the complex (**3**).

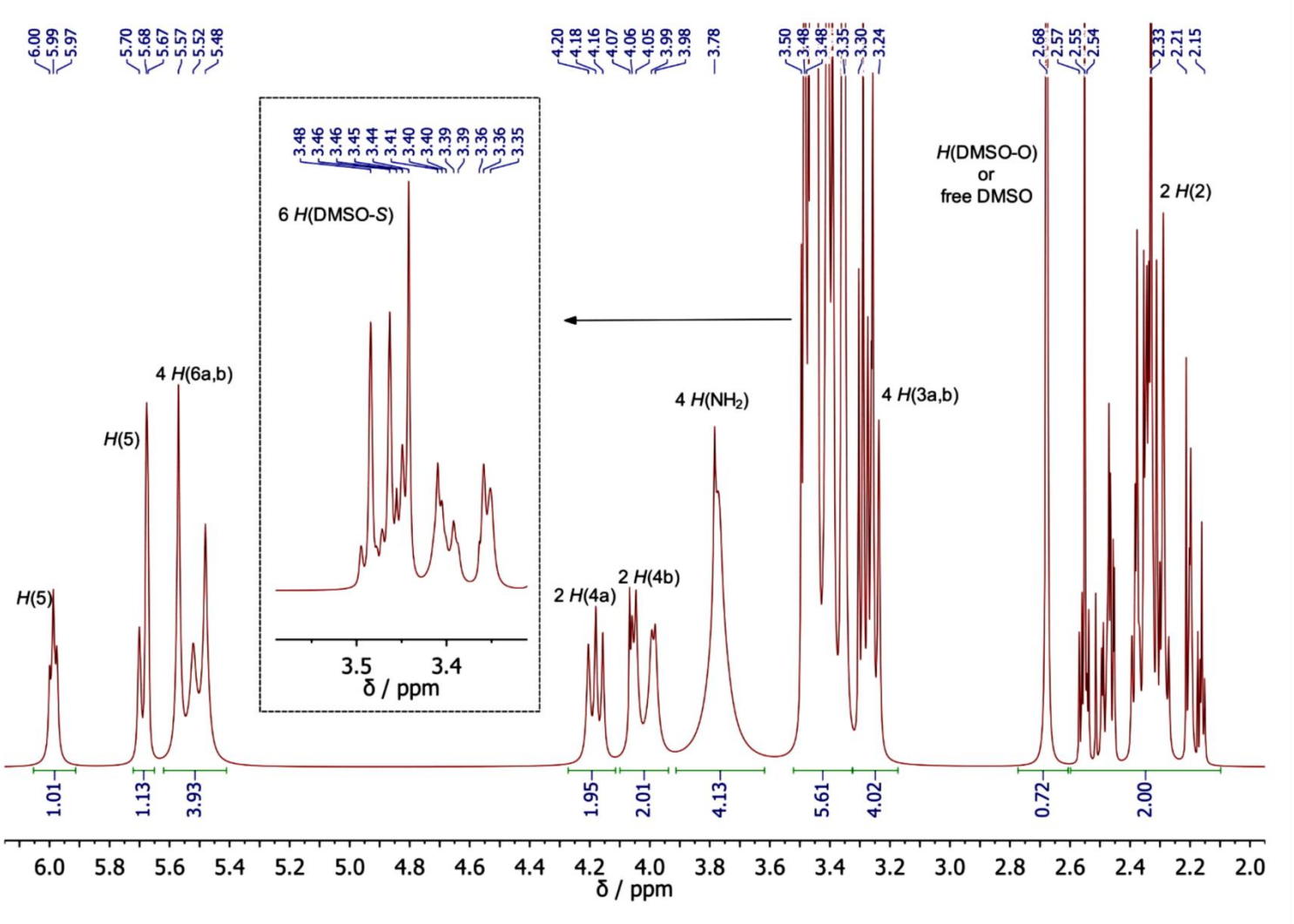

Figure S7. ^{1}H NMR spectrum of the complex (**2**).

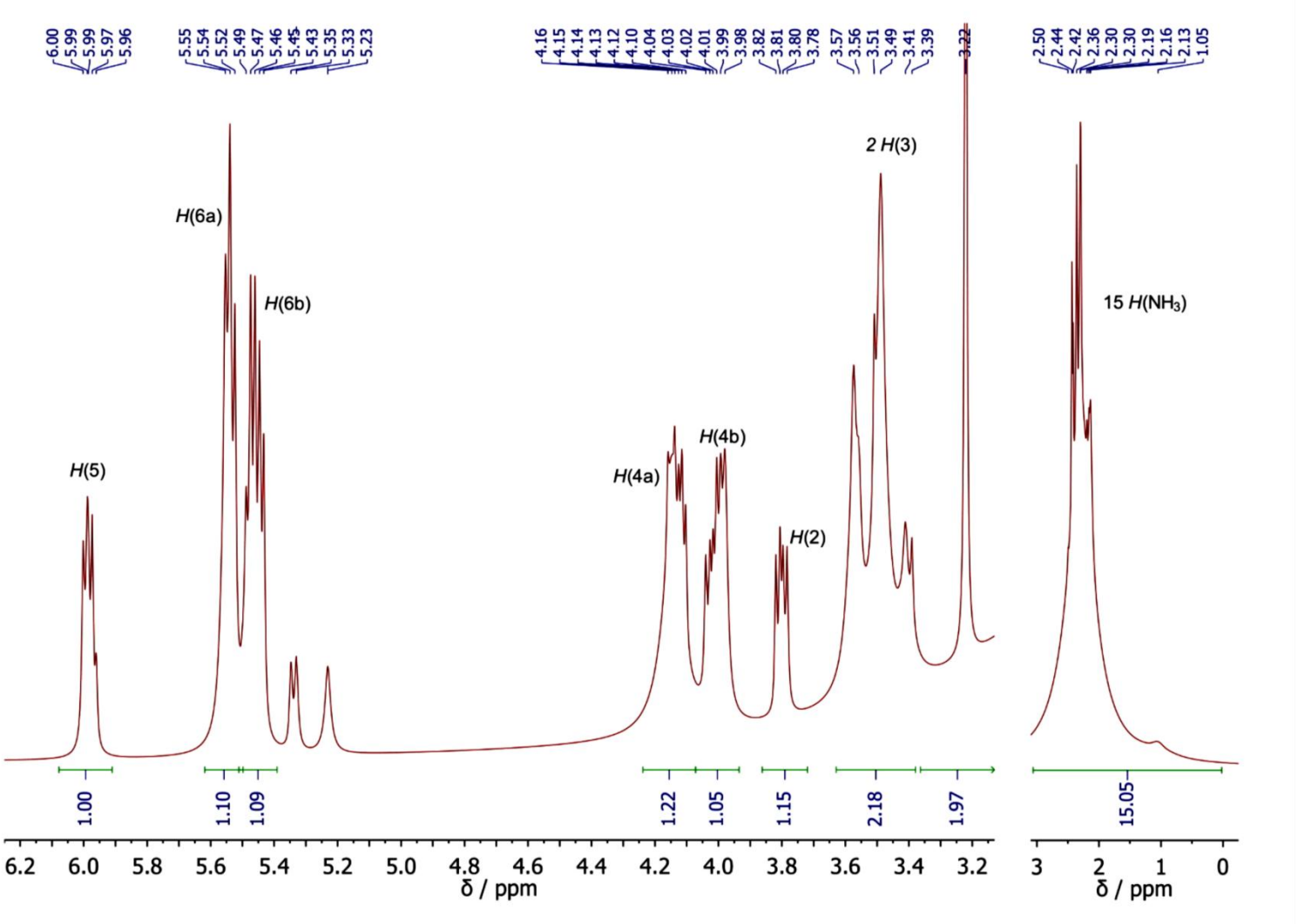

Figure S8. ^{1}H NMR spectrum of the complex (**3**).

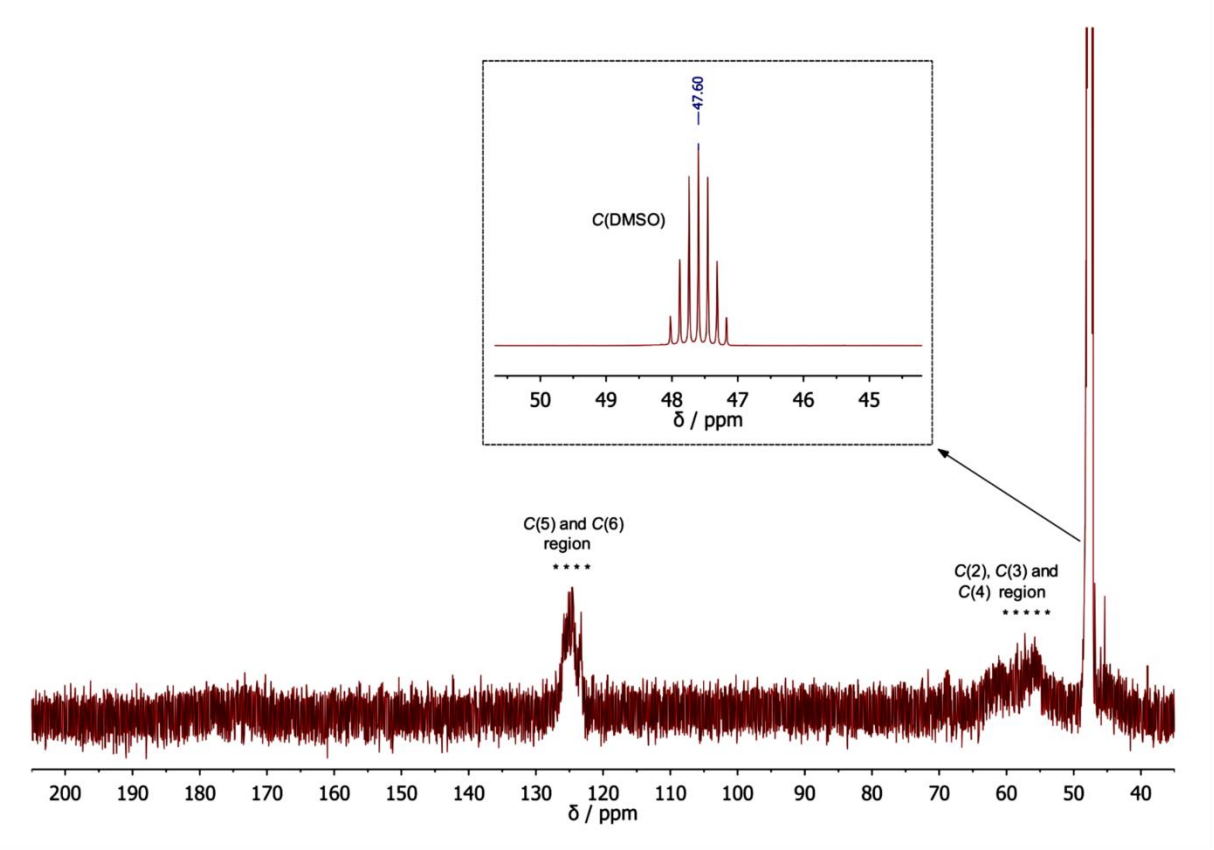

Figure S9. The ^{13}C NMR spectrum of the complex (**2**).

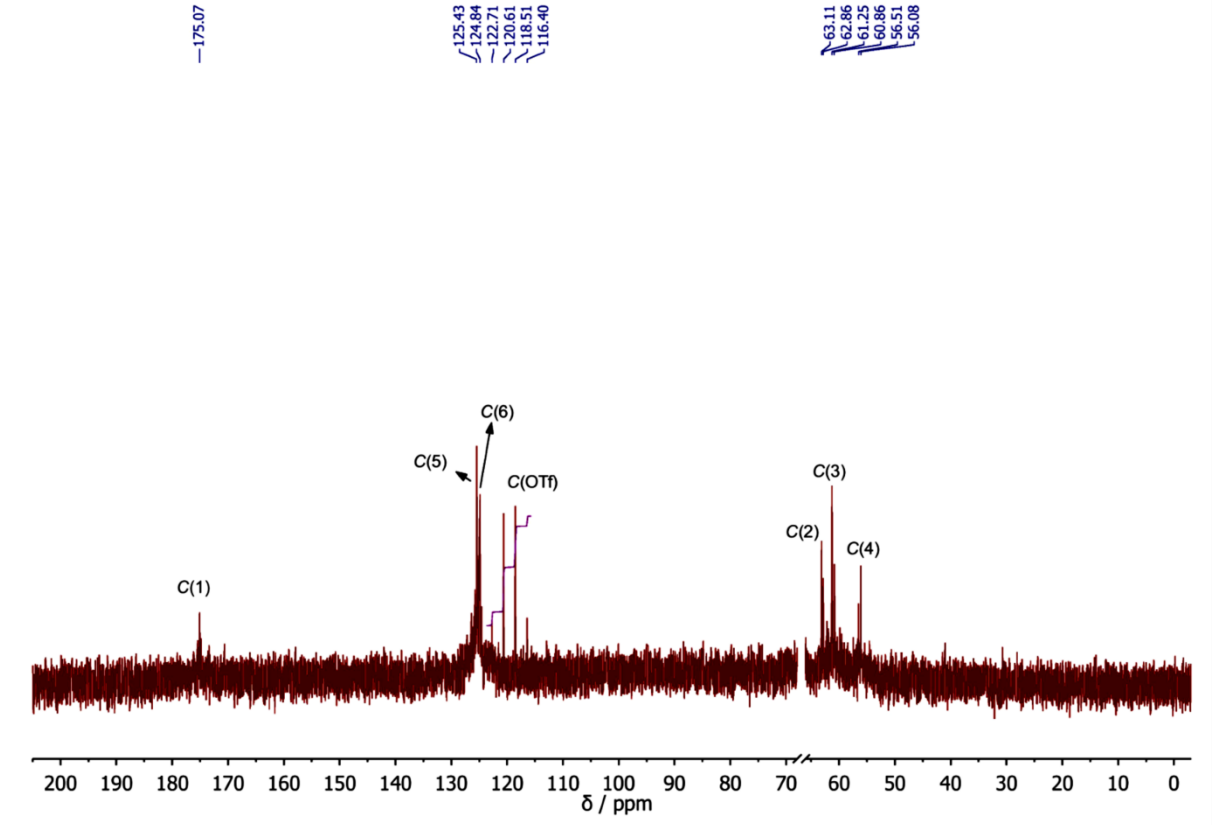

Figure S10. The ^{13}C NMR spectrum of the complex (**3**).

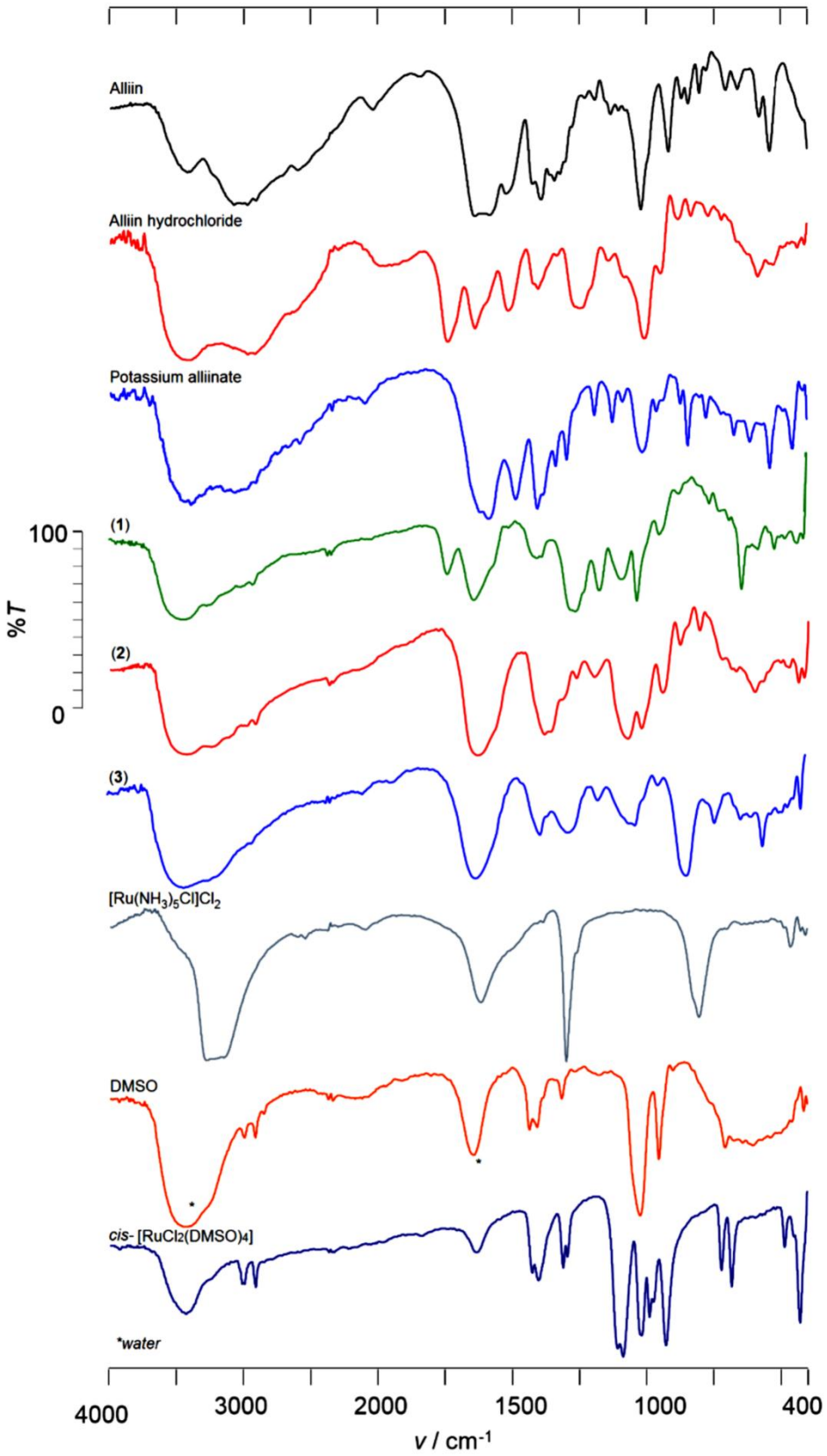

Figure S11. Infrared spectra of alliin at different protonation of amine nitrogen and carboxylate oxygen, ruthenium – alliin complexes (**1**) – (**3**) and starting ruthenium compounds.

Table S1. Positions of the bands in infrared spectra of complexes (**1**) – (**3**), starting Ru compounds and alliin.

Entry	Compound	ν_s(COOH)	ν_s (C=C)	$\nu_s(COO^-)$	$\delta_d(NH_3)$	$\delta(NH_2)$	$\delta(NH_3^+)$	$\nu_s(COO^-)$	$\delta(CH_3)$		$\delta_d(NH_3)$	ν_s(S=O) triflate	ν_s(S=O)			ν_s(C-N)	$\rho_r(NH_3)$
													S-bonded		free	O-	
1.	Alliin		1641	1611		1585	1525	1391							1021		993	
2.	Alliin hydrochloride	1740	1640				1514								1008			
3.	Potassium alliinate		1620	1620		1587	1488	1408							1015			
4.	(**1**)	1738	1640			1565	-		1404	1386		1277	1089	1032			948	
5.	(**2**)		1632	1632		1585	-	1383	1405	1383			1072		1021		943	
6.	(**3**)		1629	1629			-	1387			1287	1279			1032		998	843
7.	$[Ru(NH_3)_5Cl]Cl_2$				1630						1300							804
8.	Dimethyl sulfoxide								1436	1407					1023			
9.	*cis*-$[RuCl_2(DMSO)_4]$								1426	1401			1087			926		

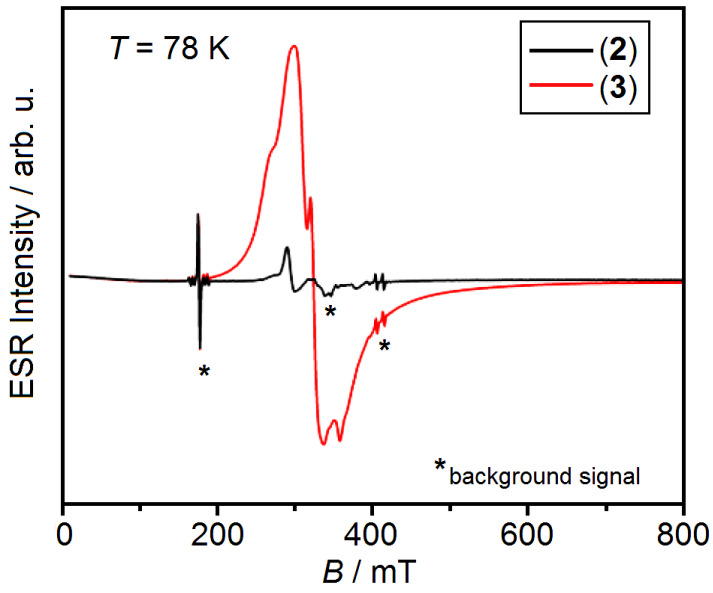

Figure S12. The comparison of ESR signals of (**2**) and (**3**).

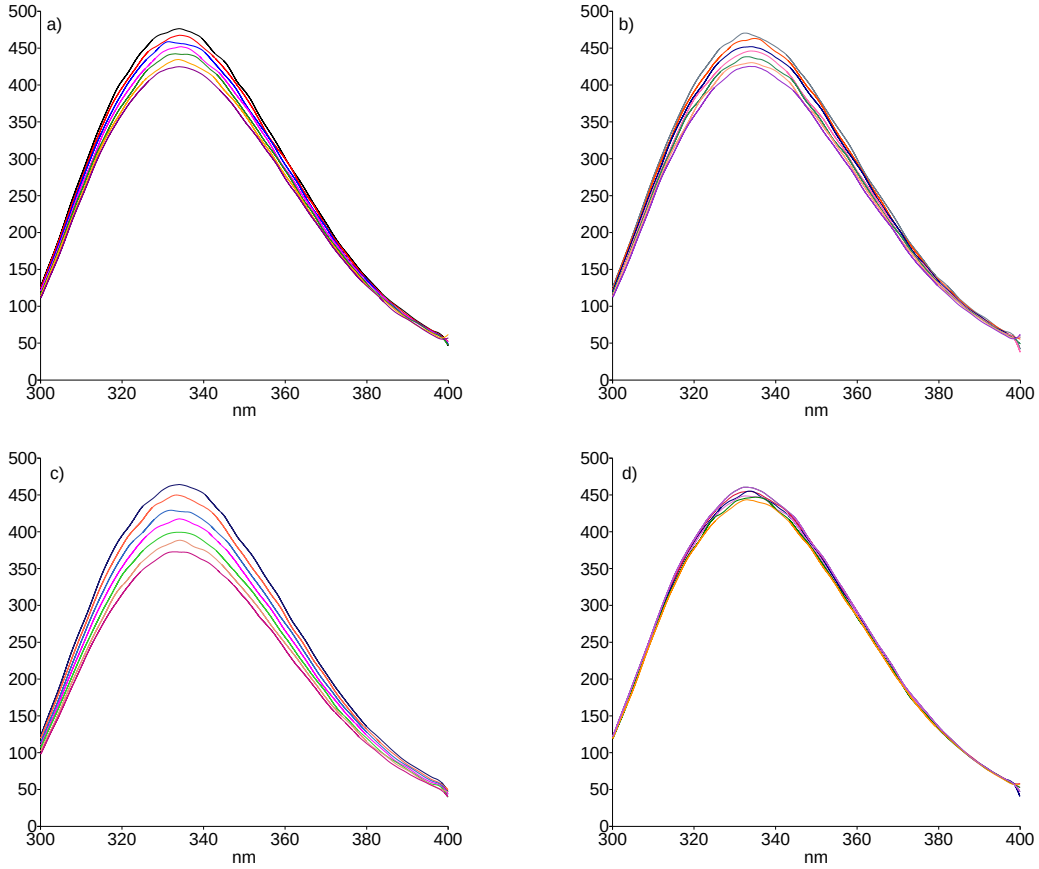

Figure S13. Quenching of the apotransferrin fluorescence in the absence and presence of increasing concentrations of (**1**) – (**3**) (a – c) and alliin (d) at 298 K.

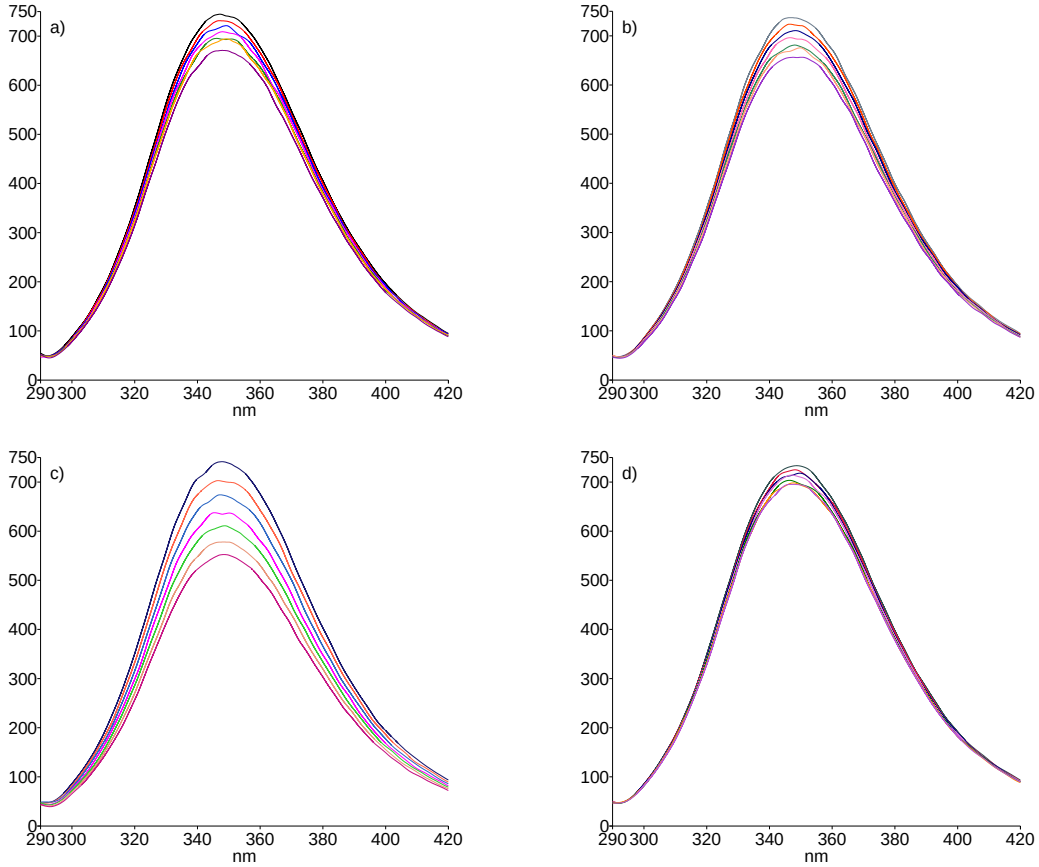

Figure S14. Quenching of BSA fluorescence in the absence and presence of increasing concentrations of (**1**) – (**3**) (a – c) and alliin (d) at 291 K.

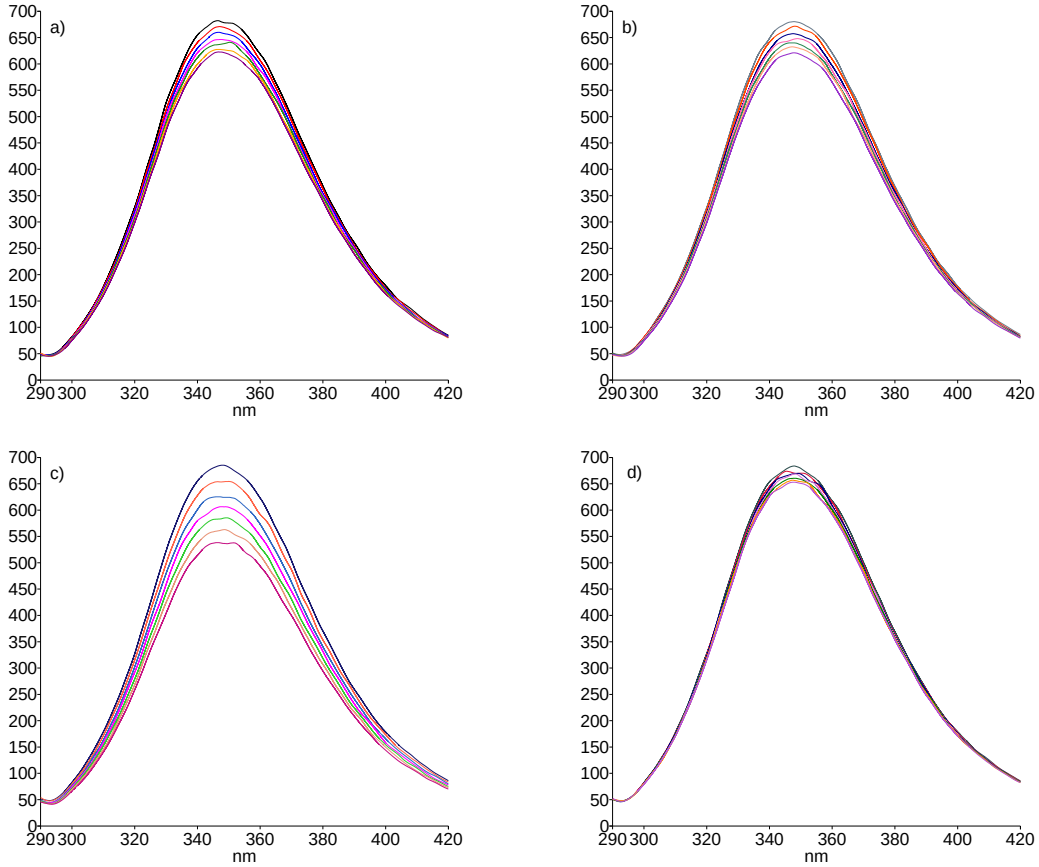

Figure S15. Quenching of BSA fluorescence in the absence and presence of increasing concentrations of (**1**) – (**3**) (a – c) and alliin (d) at 298 K.

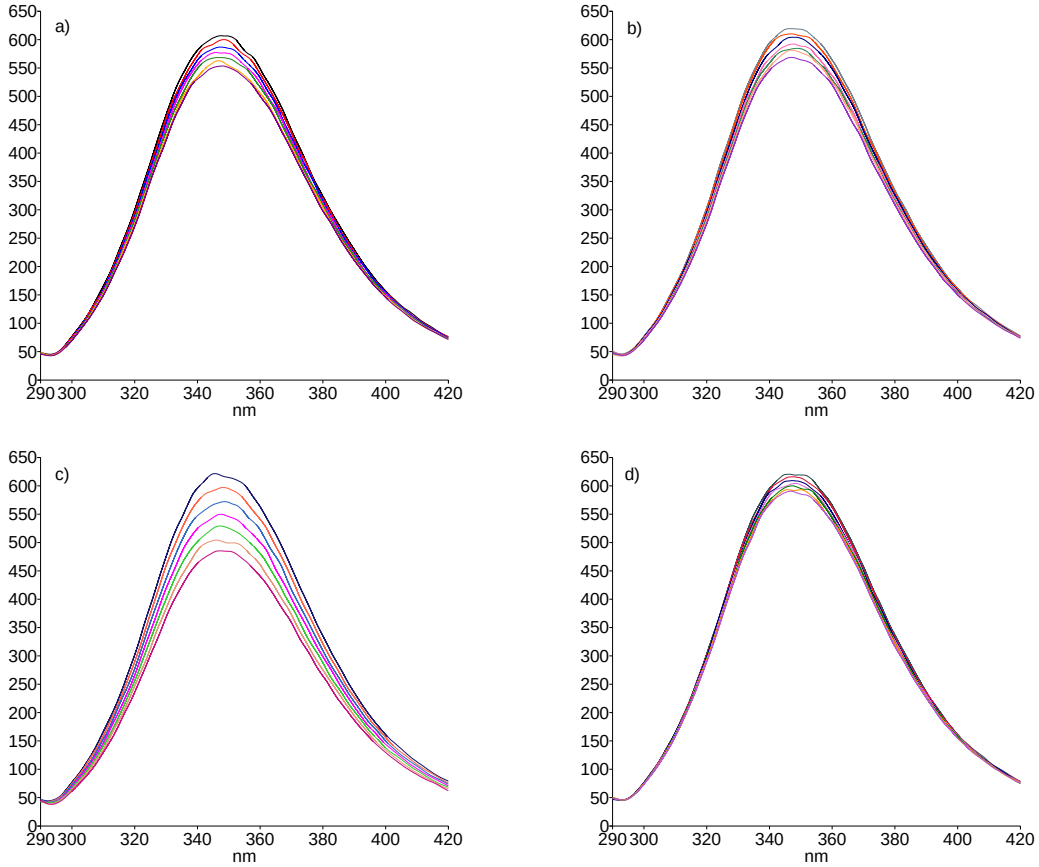

Figure S16. Quenching of BSA fluorescence in the absence and presence of increasing concentrations of (**1**) – (**3**) (a – c) and alliin (d) at 298 K.

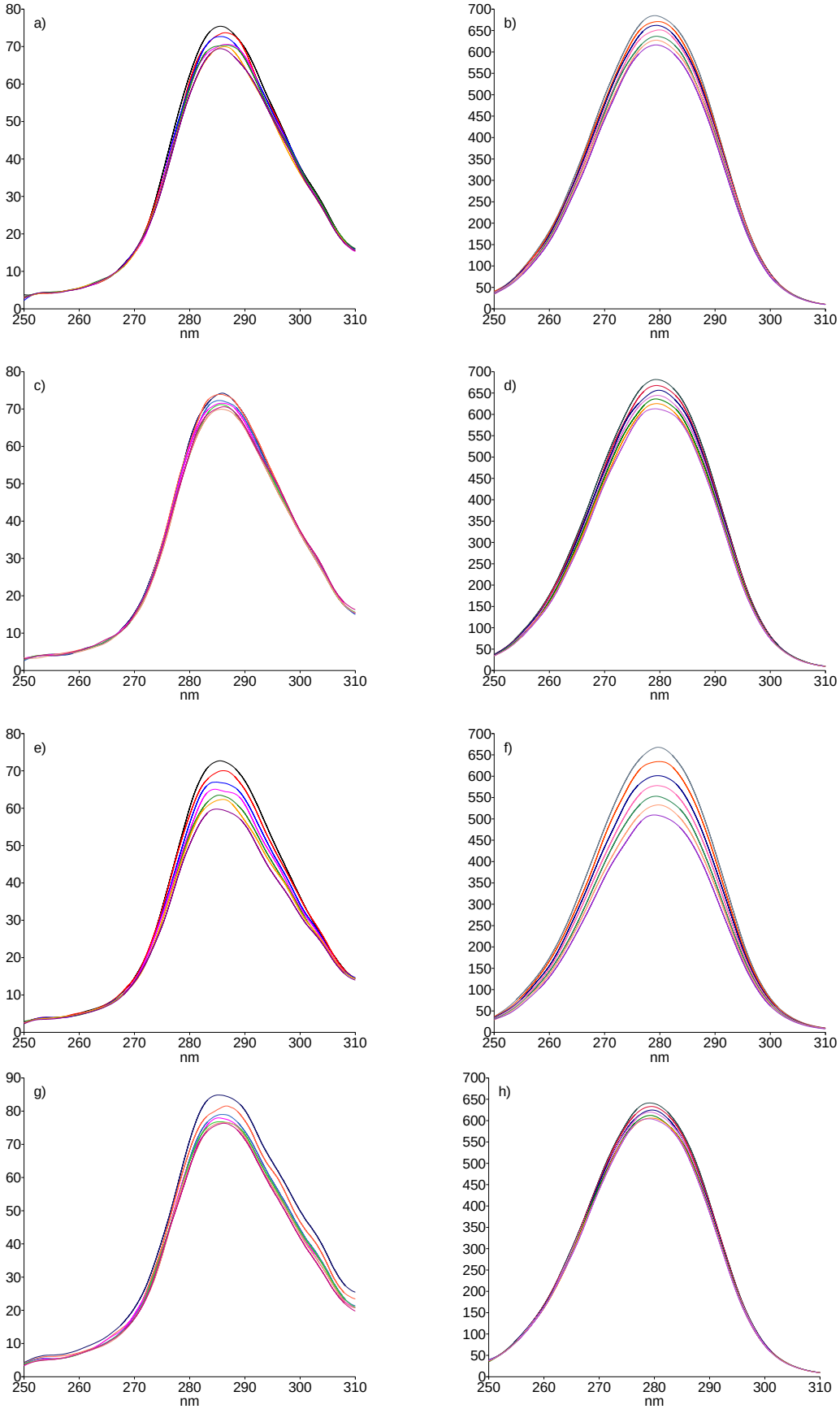

Figure S17. Synchronous fluorescence spectra of BSA in the absence and presence of increasing concentrations of complexes (**1**) (a, b), (**2**) (c, d), (**3**) (e, f) and alliin (g, h); Δλ = 15 nm (left column) and Δλ = 60 nm (right column).

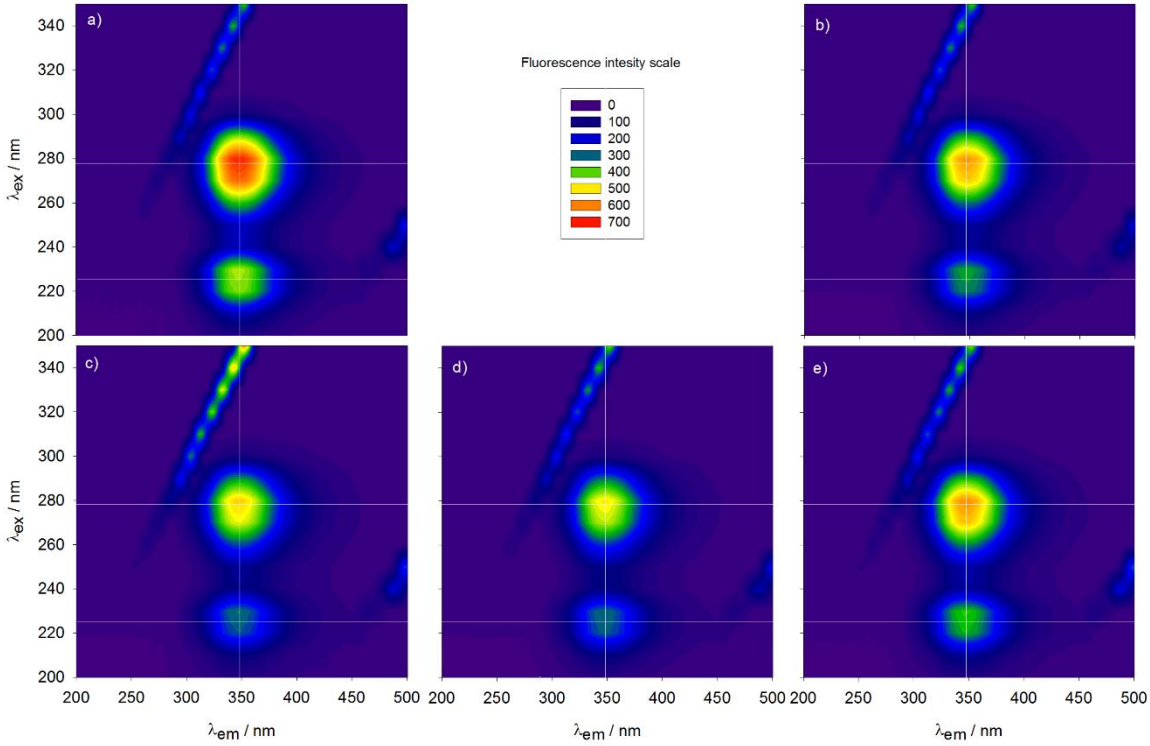

Figure S18. 2D fluorescence spectra of BSA in absence (a) and presence of complex (**1**) – (**3**) (b – d) and alliin (e). [BSA] = 1.71 µM and [complex] = 12.5 µM.

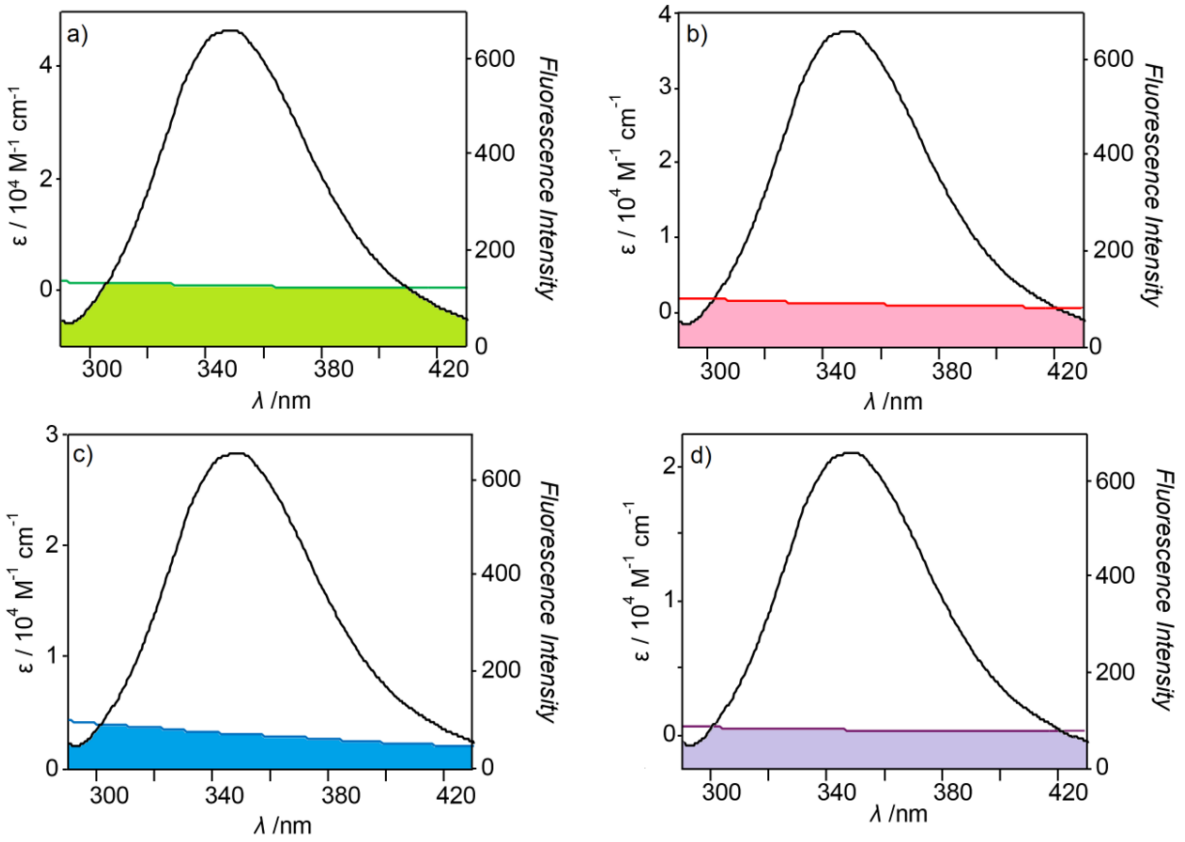

Figure S19. Overlap of the fluorescence emission spectrum of BSA and absorption spectrum of a) (**1**), b) (**2**), c) (**3**) and d) alliin.

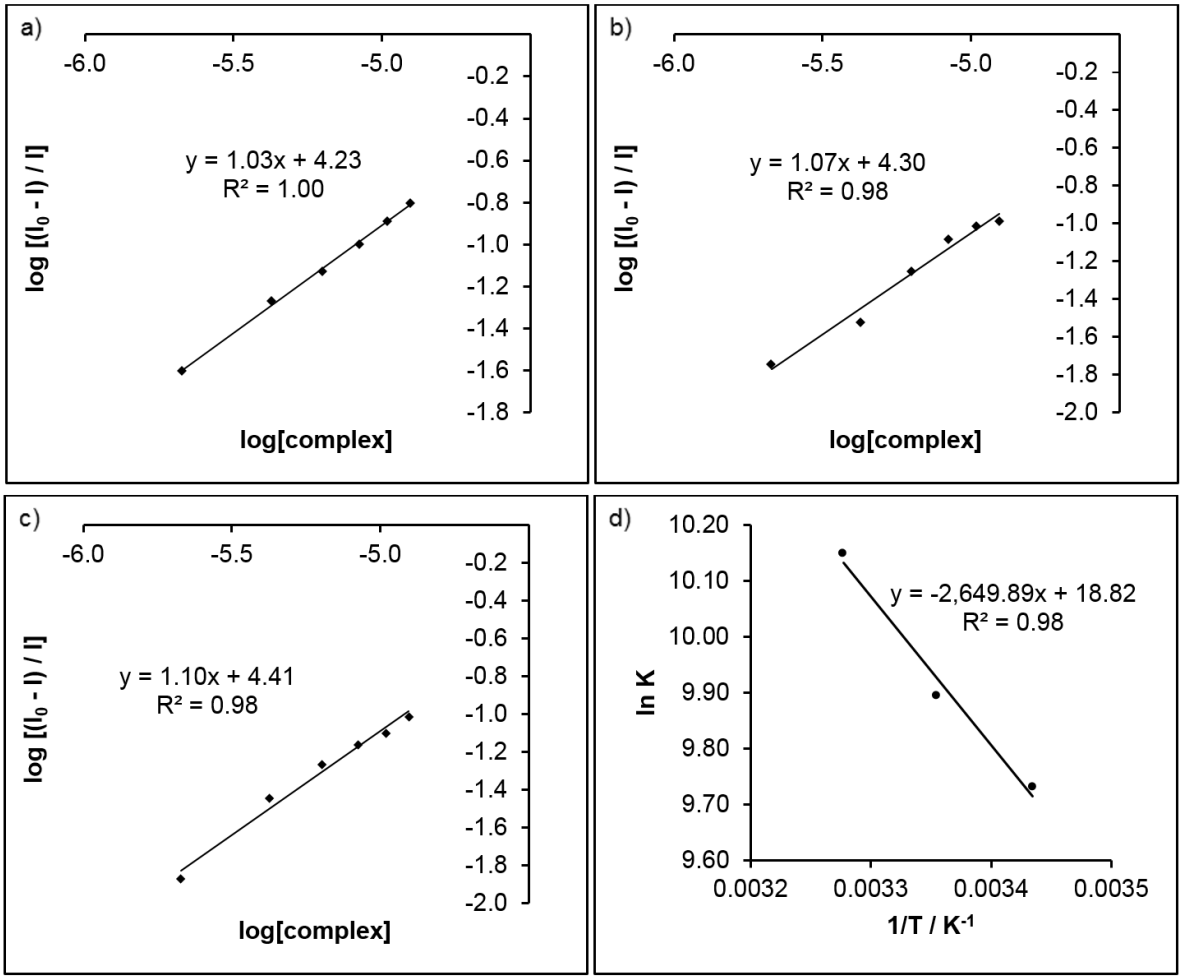

Figure S20. Graphical determination of the binding constant (K_b) and a number of binding sites (n) of complex (**1**) to BSA at three temperatures: a) 291 K, b) 298 K, c) 305 K and d) van't Hoff plot.

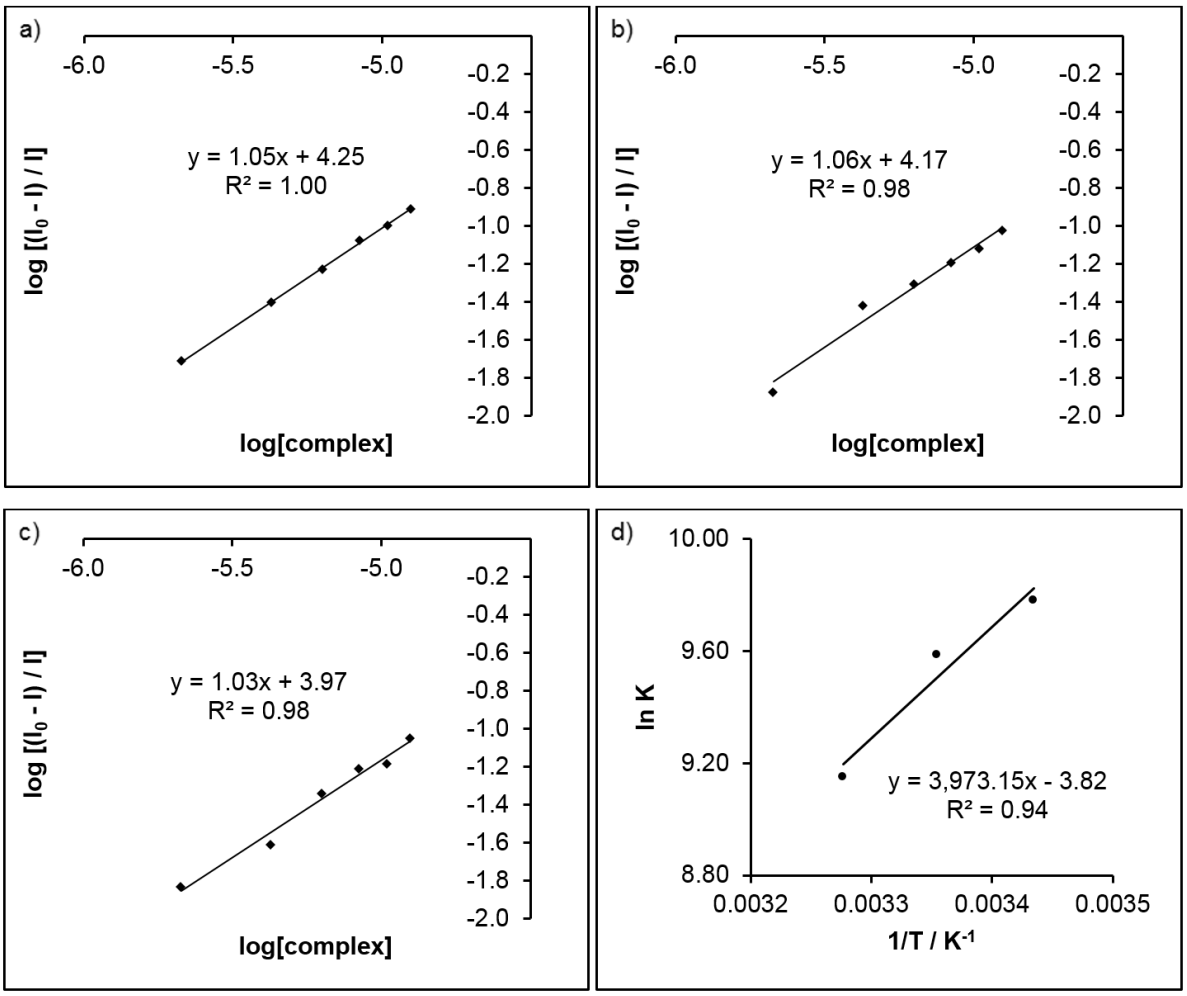

Figure S21. Graphical determination of the binding constant (K_b) and a number of binding sites (n) of complex (**2**) to BSA at three temperatures: a) 291 K, b) 298 K, c) 305 K and d) van't Hoff plot.

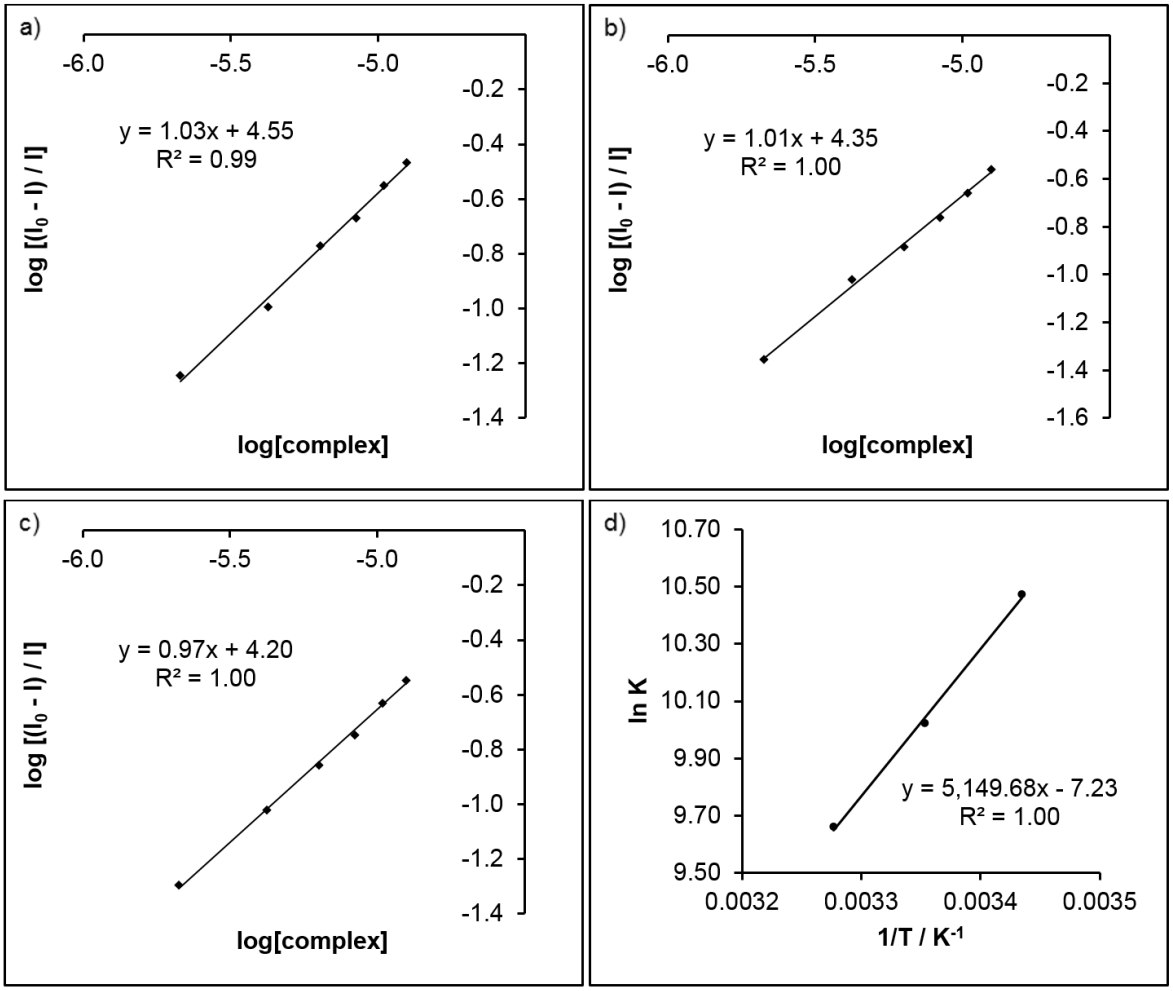

Figure S22. Graphical determination of the binding constant (K_b) and a number of binding sites (n) of complex (**3**) to BSA at three temperatures: a) 291 K, b) 298 K, c) 305 K and d) van't Hoff plot.

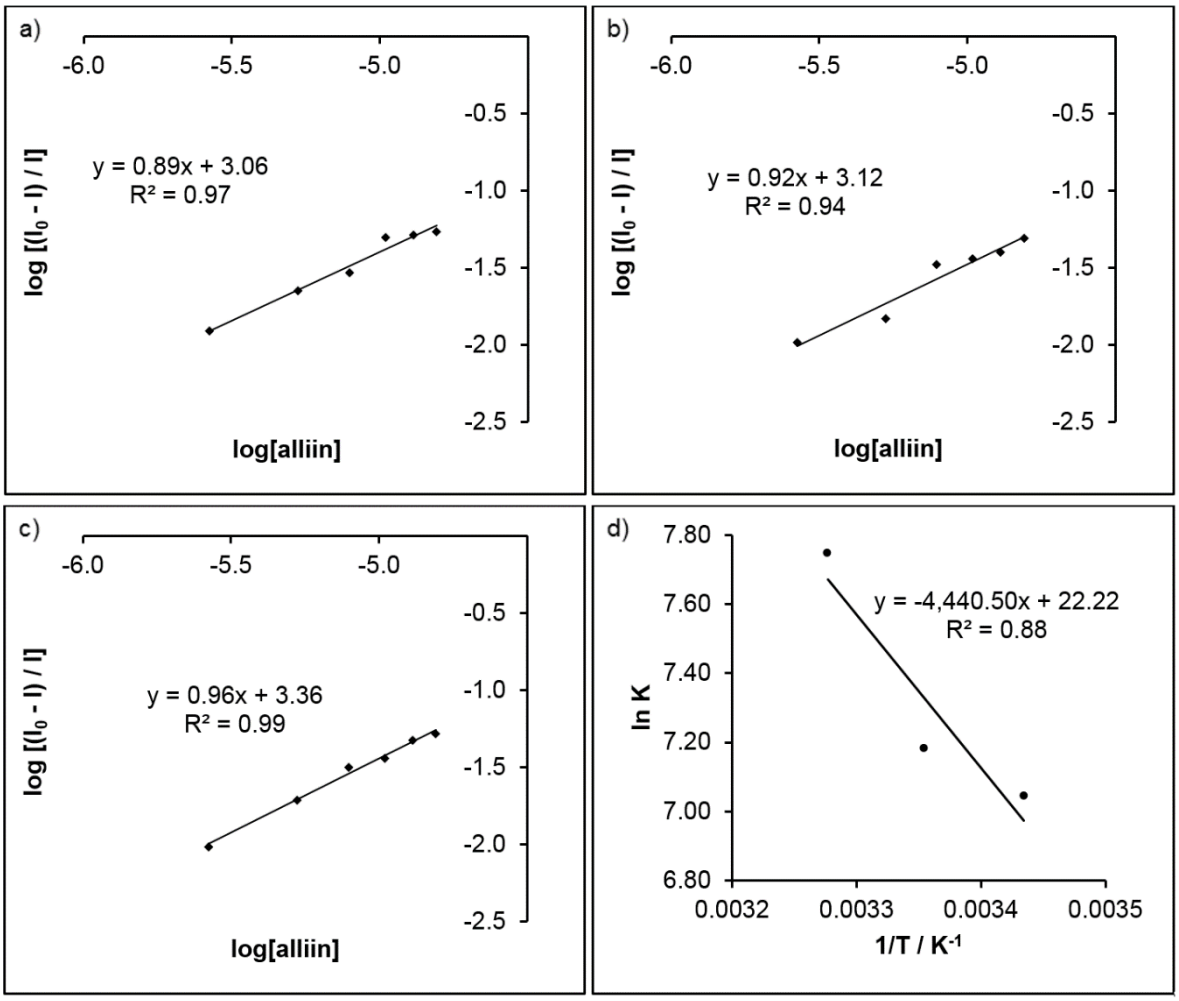

Figure S23. Graphical determination of the binding constant (K_b) and a number of binding sites (n) of alliin to BSA at three temperatures: a) 291 K, b) 298 K, c) 305 K and d) van't Hoff plot.

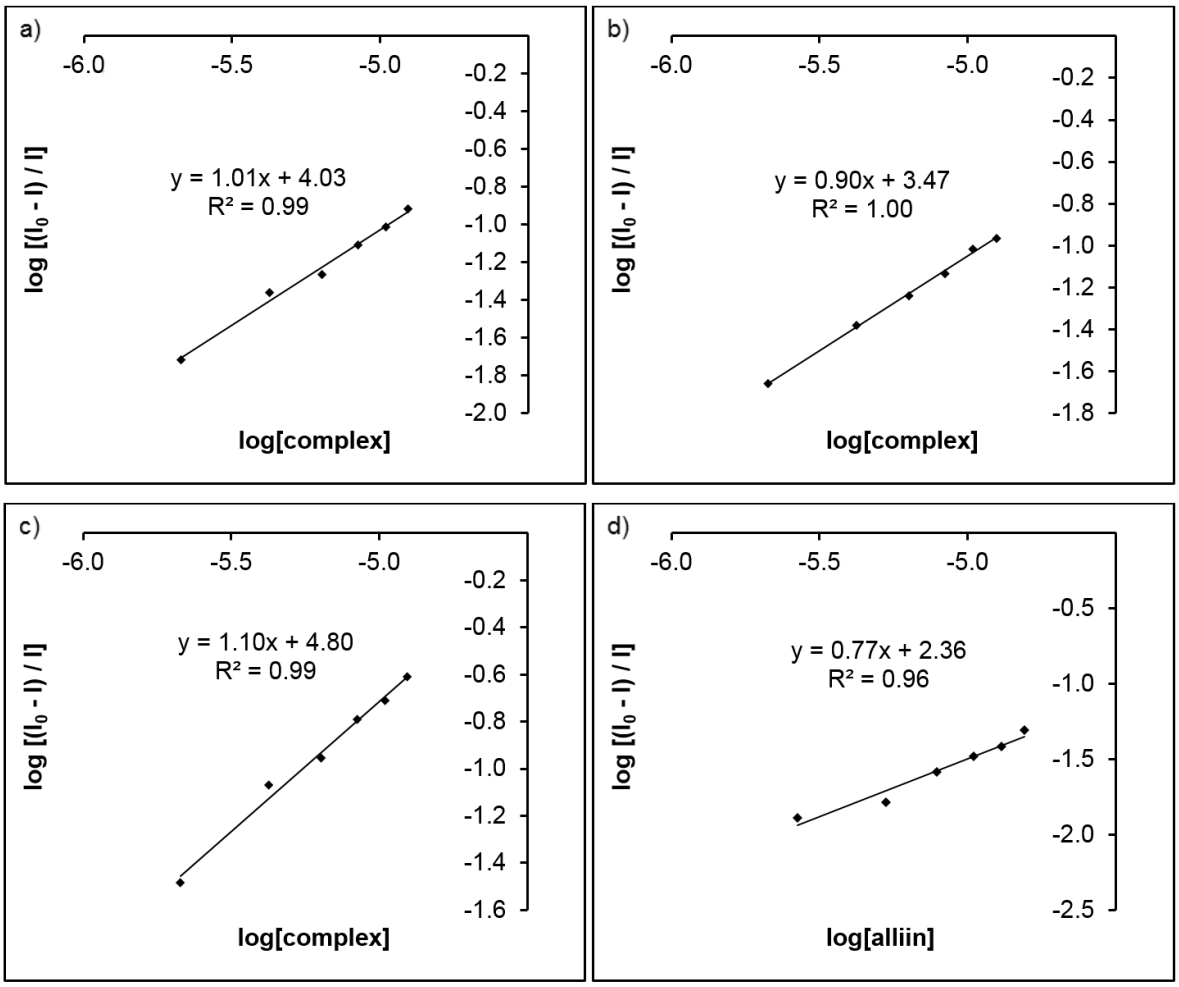

Figure S24. Graphical determination of the binding constant (K_b) and a number of binding sites (n) of complexes (**1**) – (**3**) (a – c) and alliin (d) with apotransferrin.

Proliferation assays

The panel cell lines were inoculated onto a series of standard 96-well microtiter plates on day 0, at 5000 cells per well according to the doubling times of specific cell line. Test agents were then added in five, 10-fold dilutions (0,01 to 100 µM) and incubated for further 72 hours. Working dilutions were freshly prepared on the day of testing in the growth medium. After 72 hours of incubation, the cell growth rate was evaluated by performing the MTT assay: experimentally determined absorbance values were transformed into a cell percentage growth (PG) using the formulas proposed by NIH. This method directly relies on control cells behaving normally at the day of assay because it compares the growth of treated cells with the growth of untreated cells in control wells on the same plate – the results are therefore a percentile difference from the calculated expected value.

The IC_{50} values for each compound were calculated from dose-response curves using linear regression analysis by fitting the mean test concentrations that give PG values above and below the reference value. If, however, all of the tested concentrations produce PGs exceeding the respective reference level of effect (e.g. PG value of 50) for a given cell line, the highest tested concentration is assigned as the default value (in the screening data report that default value is preceded by a ">" sign). Each test point was performed in quadruplicate in two individual experiments. The results were statistically analyzed (ANOVA, Tukey post-hoc test at $p < 0.05$). Finally, the effects of the tested substances were evaluated by plotting the mean percentage growth for each cell type in comparison to control on dose-response graphs.

Table S2. IC_{50} values for complexes (**1**) – (**3**), alliin and 5-fluorouracil.

Compound	**MCF-7**	**CFPAC-1**	**HeLa**	**SW620**	**HFF-1**
			IC_{50} / µM		
(**1**)	>100	>100	>100	>100	0.74
(**2**)	>100	>100	>100	>100	0.08
(**3**)	>100	>100	33.82*	>100*	89*
HL	>100	>100	>100	>100	19.58
5-FU**	0.096	0.25	8.62	0.075	0.94 [a]

*Unusual growth response curve

**5-fluorouracil – internal laboratory control

[a] results obtained on lung fibroblast WI38